An application of piecewise-linear holistic discretisation

G. A. Jarrad and A. J. Roberts

May 20, 2015

Abstract

The fidelity of numerical simulation of a spatio-temporal dynamical system is largely constrained by the chosen discretisation of the PDE. In particular, the modeller is typically free to choose arbitrary finite-element forms for the various spatial derivatives, without necessarily having knowledge of the accuracy of the resulting numerical schemes. The holistic discretisation approach described in this paper obviates the problem of arbitration.

Centre manifold theory is applied to derive an asymptotically accurate representation of the microscale dynamics of the one-dimensional Burgers' equation. In the process, the corresponding macroscale dynamics are constrained to match the microscale solution at discrete grid-points. The resulting representation of macroscale evolution provides an unambiguous discretisation of the PDE, suitable for numerical simulation.

The iterative process starts with a choice of the leading, macroscale approximation to the linearised system. Suitable internal boundary conditions are then induced on the spatial derivatives at the end-points of each discrete interval. Although the choice of IBCs might appear to be arbitrary, they are in fact governed by the placement of the grid-points and the form of the leading discrete approximation. The particular approach taken here is to start with a piecewise linear but continuous approximation, in contrast to similar analyses that use piecewise constant, discontinuous approximations. This is motivated by the principle that a more accurate leading approximation should lead to faster convergence of the asymptotic solution, via the Rayleigh-Ritz theorem.

Further iterations of the centre manifold process lead inexorably to a temporal evolution formulation of the macroscale dynamics, holistically informed by the underlying microscale dynamics. We examine

the accuracy and stability of the resulting numerical scheme, in comparison to the behaviours of several other typical approximations.

1   Introduction

As an application of holistic discretisation, consider the numerical simulation of a field $u(x, t)$ of the nonlinear advection–diffusion Burgers' PDE

$$\frac{\partial u}{\partial t} = \nu \frac{\partial^2 u}{\partial x^2} - \alpha u \frac{\partial u}{\partial x}. \tag{1.1}$$

The spatial domain $\mathbb{X}$ is of length L, $0 \leq x \leq L$, and we consider solutions L-periodic in space. The first step is to discretise $\mathbb{X}$ into N equi-spaced intervals bounded by $N + 1$ grid-points X_j, $j = 0, \ldots, N$, with spacing H. The continuum dynamics of the field $u(x, t)$ are now summarised by the coarse dynamics $\vec{U} = (U_1, U_2, \ldots, U_N)$, where $U_j(t) := u(X_j, t)$ for all $t \in \mathbb{T}$.

The next step is to specify the explicit form of the coarse temporal evolution

$$\dot{\vec{U}}(t) = \vec{g}(\vec{U}(t)). \tag{1.2}$$

The traditional approach is to use centred approximations, for example, $\delta^2 U_j / H^2$ for $\partial^2 u / \partial x^2$ and $U_j \mu \delta U_j / H$ for $u \partial u / \partial x$, where $\delta = \sigma^{\frac{1}{2}} - \sigma^{-\frac{1}{2}}$, $\mu = (\sigma^{\frac{1}{2}} + \sigma^{-\frac{1}{2}})/2$, and $\sigma U_j = U_{j+1}$. However, the advection term has another plausible representation, namely the conservative form $\mu \delta U_j^2 / 2H$. For illustrative purposes, a mixture of the two latter representations will be used for comparison, namely

$$\dot{U}_j = \nu \frac{\delta^2 U_j}{H^2} - (1 - \theta) \alpha \frac{U_j \mu \delta U_j}{H} - \theta \alpha \frac{\mu \delta U_j^2}{2H}. \tag{1.3}$$

In contrast, the holistic approach has no such representational ambiguity, and, as shown in Section 4, gives rise at first-order to the model

$$\dot{U}_j = S \left(\nu \frac{\delta^2 U_j}{H^2} - \alpha \frac{U_j \mu \delta U_j}{3H} - \alpha \frac{\mu \delta U_j^2}{3H} \right), \tag{1.4}$$

where $S = (1 + \delta^2/6)^{-1}$. Observe that, apart from the non-local corrective operator S, this holistic model matches the mixture model (1.3) for $\theta = \frac{2}{3}$. This parameter value is exactly the critical value predicted by Fornberg (1973) to be necessary for stable simulation (with $\nu = 0$ and $\alpha = 1$) for a selection of numerical integration schemes. Further comparisons of the numerical behaviours of the holistic and mixture models are given in Section 5.

The final step in the simulation process is to interpolate from the coarse solution $\vec{U}(t)$ back to the continuum field $u(x,t)$ via a spatial mapping of the form

$$u(x,t) = \hat{u}(x, \vec{U}(t)).\tag{1.5}$$

The complete holistic framework comprises equations (1.2) and (1.5), along with the addition of suitable boundary conditions that are discussed in Section 3. We show in Section 4 that, to first-order, the holistic mapping $\hat{u}$ takes the form

$$\hat{u} = \sum_{j=1}^{N} \chi_j \left(\mathcal{I}_0 U_j + \frac{H^2}{6}\mathcal{I}_1 \dot{U}_j + \alpha\frac{H}{6}\mathcal{I}_1 U_j \cdot (1 - \sigma^{-1})U_j \right),\tag{1.6}$$

using the interpolation operators $\mathcal{I}_0 = \xi + (1 - \xi)\sigma^{-1}$ and $\mathcal{I}_1 = \xi^3 + (1 - \xi)^3\sigma^{-1} - \xi(1 - \sigma^{-1}) - \sigma^{-1}$, where $\xi = \sum_{j=1}^{N} \chi_j \xi_j$ with $\xi_j(x) = (x - X_{j-1})/H$ and $\chi_j(x) = 1$ (else 0) for $X_{j-1} \leq x < X_j$.

2 Motivation

The choice of a piecewise linear leading approximation, in contrast to the usual piecewise constant one (Roberts 2001, 2003, Roberts et al. 2014), is motivated by an application of the Rayleigh–Ritz theorem. Consider a general dynamical system of the form

$$\dot{\vec{u}} = \mathcal{L}\vec{u} + \mathcal{N}(\vec{u}),\tag{2.1}$$

where it is pre-supposed for convenience that $\mathcal{N}(\vec{0}) = \vec{0}$. The slow manifold approximation to the dynamics of the linearised system

$$\dot{\vec{u}} = \mathcal{L}\vec{u}\tag{2.2}$$

about $\vec{u} = \vec{0}$ is then parameterised as

$$\vec{u} = V\vec{s}, \qquad \dot{\vec{s}} = \Lambda\vec{s},\tag{2.3}$$

whereupon $V\Lambda\vec{s} = \mathcal{L}V\vec{s}$ for arbitrary $\vec{s}$. Observe now that a particular choice of $\Lambda = \mathrm{diag}(\lambda_1, \lambda_2, \ldots)$ uncouples this relation into the components $\mathcal{L}\vec{v}_j = \lambda\vec{v}_j$, where $V = [\vec{v}_1, \vec{v}_2, \ldots]$.

Now, when $\mathcal{L}$ is self-adjoint, the Rayleigh–Ritz theorem is that $\lambda_j = R(\vec{v}_j)$ for the Rayleigh quotient

$$R(\vec{v}) = \frac{\langle \vec{v}, \mathcal{L}\vec{v} \rangle}{\|\vec{v}\|^2}.$$

3

It can further be shown, upon perturbing $\vec{v}_j$ to $\vec{u} = \vec{v}_j + \epsilon \vec{w}$, that $R(\vec{u}) = \lambda_j + O(\epsilon^2)$. The slow manifold is based upon the slow subspace spanned by the slow eigenvectors, and the evolution on the slow manifold corresponds to eigenvalues of the linearisation. Hence the Rayleigh–Ritz quotient suggests that the more accurate we make a linear subspace approximation to the field $u(x,t)$, the more accurate the evolution on the slow manifold. Consequently, Section 3 develops a piecewise linear and continuous subspace approximation to the field, instead of the piecewise constant and discontinuous approximation developed previously (Roberts 2001, 2003, Roberts et al. 2014).

3 Linear analysis

Burgers' equation (1.1) linearises to equation (2.2) for $\alpha = 0$, with the linear operator $\mathcal{L} = \nu \partial^2 / \partial x^2$. It can be shown that $\mathcal{L}$ is self-adjoint under any of these external boundary conditions: L-periodic; Dirichlet ($u(0,t) = u(L,t) = 0$); or Neuman ($u_x(0,t) = u_x(L,t) = 0$). We have chosen the first condition for convenience. The linear system has two eigenmodes corresponding to eigenvalue $\lambda = 0$, namely

$$v = 1\,, \qquad v = x\,, \tag{3.1}$$

and general eigenmodes for $\lambda = -\nu k^2 < 0$ of the form

$$v = e^{-\nu k^2 t \pm ikx}\,. \tag{3.2}$$

Hence, any peicewise–linear approximation to u is an equilibrium solution of the linearised system. We choose a continuous approximation that is aligned at the internal grid-points $X_j = jH$, $j = 1, 2, \ldots, N-1$, namely

$$\hat{u}_0 = \sum_{j=1}^N \chi_j (\xi U_j + (1-\xi)U_{j-1})\,, \tag{3.3}$$

with indicator $\chi_j(x) = 1$ (else 0) for $X_{j-1} \le x < X_j$, and dimensionless coordinate $\xi(x) = \sum_{j=1}^N \chi_j(x)(x - X_{j-1})/H$. This enforced continuity is represented by internal boundary conditions (IBCs) of the form

$$[\hat{u}]_j = 0 \qquad \text{for } j = 1, 2, \ldots, N-1\,, \tag{3.4}$$

where $[u]_j := \lim_{\epsilon \to 0^+} u(X_j + \epsilon, t) - u(X_j - \epsilon, t)$ represents the spatial jump in u across the boundary between the j-th and $(j+1)$-th intervals.

Unfortunately, this continuity does not hold for the first spatial derivative, since it can be shown that $[\partial \hat{u}_0 / \partial x]_j = \delta^2 U_j / H$. Hence, we introduce a homotopic smoothing parameter γ $(0 \leq \gamma \leq 1)$, and enforce the additional IBCs:

$$[\hat{u}_x]_j = \frac{1 - \gamma}{H}\, \delta^2 \hat{u}\big|_{X_j} \qquad \text{for } j = 1, 2, \ldots, N - 1 \,, \tag{3.5}$$

such that smooth approximations are found in the limit as $\gamma \to 1$. Consequently, the state-space is now extended to (u, α, γ), for which $(\hat{u}_0, 0, 0)$ is an equilibrium of equation (1.1).

We now demonstrate that the system will be robust to nonlinear perturbations about this equilibrium. We seek the spatial stability over $\mathbb{X}$ of the eigenmode

$$v = \sum_{j=1}^{N} \chi_j \Re \left(a_j e^{i\kappa\xi} \right) \,, \tag{3.6}$$

for some fixed, nondimensionalised wavenumber $\kappa = kH$, and arbitrary, time–varying coefficients $a_j = A_j + iB_j$. The continuity condition (3.4) now implies that

$$\Re \left(a_{j+1} - a_j e^{i\kappa} \right) = 0 \,. \tag{3.7}$$

Similarly, the smoothness condition (3.5) implies that

$$-\kappa \Im \left(a_{j+1} - a_j e^{i\kappa} \right) = (1 - \gamma)\Re \left(a_{j+1} e^{i\kappa} + a_j - 2a_j e^{i\kappa} \right) \,. \tag{3.8}$$

In coefficient form, the update from the j-th to $(j + 1)$-th interval is

$$\begin{bmatrix} 1 & 0 \\ fc & 1 - fs \end{bmatrix} \begin{bmatrix} A_{j+1} \\ B_{j+1} \end{bmatrix} = \begin{bmatrix} c & -s \\ s + f(2c - 1) & c - 2fs \end{bmatrix} \begin{bmatrix} A_j \\ B_j \end{bmatrix} \,, \tag{3.9}$$

where $c + is = e^{i\kappa}$ and $f = (1 - \gamma)/\kappa$. Putting $a_{j+1} = \mu a_j$ then leads to the characteristic equation

$$\mu^2 - 2\frac{c - fs}{1 - fs}\mu + 1 = 0 \,, \tag{3.10}$$

with characteristic roots given by

$$\mu = \beta \pm \sqrt{\beta^2 - 1} \quad \text{for } \beta = \frac{c - fs}{1 - fs} \leq 1 \,. \tag{3.11}$$

Consequently, there are three distinct stability regimes governed by β:

1. $|\beta| < 1$, which gives rise to complex roots with $|\mu| = 1$ (*stable*). This includes the limiting case of $\gamma = 1$ ($f = 0$), for which $\mu = c \pm is = e^{\pm i\kappa}$.

2. $\beta = \pm 1$, corresponding to $\kappa = n\pi$, $n = 0, 1, 2, \ldots$, which gives rise to a repeated, real root of $\mu = \pm 1$ (*stable*).

3. $\beta < -1$, which gives rise to the two real roots $\mu < -1$ and $-1 < \mu < 0$ (*saddle unstable*).

The $\beta < -1$ regime comprises small regions of instability near $\kappa = (2n + 1)\pi$, $n = 0, 1, 2, \ldots$, for which the eigenmode cannot persist unattenuated throughout space. It can be shown that these forbidden regions obey

$$\frac{\kappa}{2} < (1 - \gamma)\tan\frac{\kappa}{2}, \qquad \kappa \neq n\pi. \tag{3.12}$$

Thus, at equilibrium ($\gamma = 0$) there is an initial forbidden gap $\kappa \in (0, \pi)$ adjacent to the centre manifold wavenumber $\kappa = 0$ (see Figure 3.1), indicating that transient solutions decay to the centre manifold at a rate of at least $\lambda = -\nu k^2 = -\frac{\nu \pi^2}{H^2}$. It is this gap that provides robustness to nonlinear perturbations about the equilibrium within some suitable region in state-space.
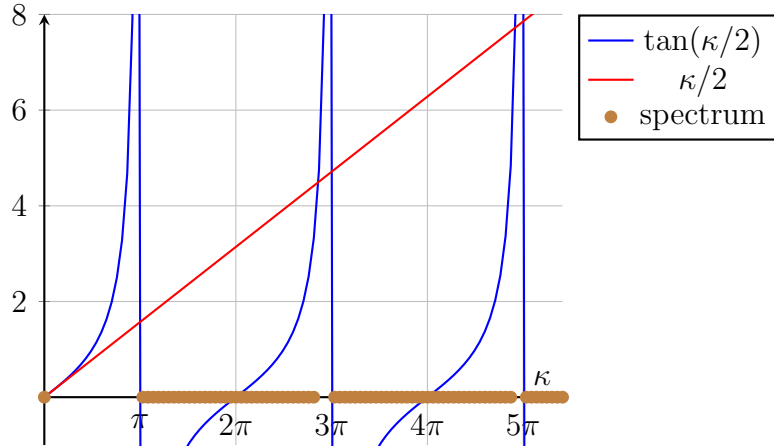

Figure 3.1: The equilibrium ($\gamma = 0$, $\alpha = 0$) spectrum determined by the forbidding condition (3.12). The thick lines along the κ-axis indicate regions of wavenumbers for which the corresponding eigenmodes are stable.

4 Nonlinear analysis

With the aid of holistic equations (1.2) and (1.5), viz $u = \hat{u}$ and $\dot{\vec{U}} = \vec{g}$, we rewrite Burgers' equation (1.1) in the form

$$\mathcal{M}(\hat{u}, \vec{g}) = \mathcal{L}\hat{u} - \frac{\partial \hat{u}}{\partial \vec{U}} \cdot \vec{g} - \alpha \hat{u} \hat{u}_x = 0 \,, \tag{4.1}$$

where $\mathcal{L} = \nu \partial^2 / \partial x^2$ from Section 3. The linear analysis of that section is now extended by considering perturbations about the equilibrium $(\hat{u}, \gamma, \alpha) = (\hat{u}_0, 0, 0)$. In particular, consider the power series

$$\hat{u} \sim \sum_{p=0}^{\infty} \sum_{q=0}^{\infty} \gamma^p \alpha^q \hat{u}^{(p,q)} \,, \qquad \vec{g} \sim \sum_{p=0}^{\infty} \sum_{q=0}^{\infty} \gamma^p \alpha^q \vec{g}^{(p,q)} \,, \tag{4.2}$$

where $\hat{u}^{(0,0)} = \hat{u}_0$ and $\vec{g}^{(0,0)} = 0$. Substituting these expansions into equation (4.1), the terms $\hat{u}^{(p,q)}$ and $\vec{g}^{(p,q)}$ are computed subject to the IBCs (3.4) and (3.5).

To simplify this process algebraically, we follow the approach of Jarrad: without loss of generality, consider finite truncations of the power series subject to $p + q \leq n$, namely[1]

$$\hat{u}^{<n>} = \sum_{p=0}^{n} \sum_{q=0}^{n-p} \gamma^p \alpha^q \hat{u}^{(p,q)} \,, \qquad \hat{u}_n = \sum_{p=0}^{n} \gamma^p \alpha^{n-p} \hat{u}^{(p,n-p)} \,. \tag{4.3}$$

Letting $\varepsilon^2 = \gamma^2 + \alpha^2$ for convenience[2], we obtain $\hat{u} = \hat{u}^{<n>} + O(\varepsilon^{n+1})$ and $\hat{u}^{<n>} = \hat{u}^{<n-1>} + \hat{u}_n$; likewise for $\vec{g}^{<n>}$ and $\vec{g}_n$. It can then be shown that

$$\mathcal{M}(\hat{u}^{<n>}, \vec{g}^{<n>}) = \mathcal{L}\hat{u}_n - \frac{\partial \hat{u}_0}{\partial \vec{U}} \cdot \vec{g}_n + \mathcal{M}(\hat{u}^{<n-1>}, \vec{g}^{<n-1>}) + O(\varepsilon^{n+1}) \,, \tag{4.4}$$

and hence the process is to iteratively solve

$$\mathcal{M}(\hat{u}^{<n>}, \vec{g}^{<n>}) = 0 + O(\varepsilon^{n+1}) \,, \tag{4.5}$$

or, equivalently,

$$\mathcal{L}\hat{u}_n = \frac{\partial \hat{u}_0}{\partial \vec{U}} \cdot \vec{g}_n - \mathcal{M}(\hat{u}^{<n-1>}, \vec{g}^{<n-1>}) + O(\varepsilon^{n+1}) \,. \tag{4.6}$$

---

[1] In practice, other truncation schemes may be used; for example, rectangular truncation: $p \leq n$, $q \leq m$.

[2] This is merely an algebraic device; in practice, γ and α need not be commensurate

Given $\hat{u}_0 = \sum_{j=1}^{N} \chi_j(\xi + (1-\xi)\sigma^{-1})U_j$ where $\xi = \sum_{j=1}^{N} \chi_j(x - X_{j-1})/H$, the first-order pertubation terms can now be computed for $n = 1$. Defining $\Delta = 1 - \sigma^{-1}$, observe that

$$\nu\hat{u}_1'' = \sum_{j=1}^{N} \chi_j \left[(\xi + (1-\xi)\sigma^{-1})g_{1,j} + \alpha(\xi + (1-\xi)\sigma^{-1})U_j.\frac{1}{H}\Delta U_j \right]. \quad (4.7)$$

Hence, spatially integrating twice gives

$$\nu\hat{u}_1 = \sum_{j=1}^{N} \chi_j \left[d_j + H\xi c_j + \frac{H^2}{6}(\xi^3 + (1-\xi)^3\sigma^{-1})g_{1,j} \right.$$
$$\left. + \frac{\alpha H}{6}(\xi^3 + (1-\xi)^3\sigma^{-1})U_j.\Delta U_j \right]. \quad (4.8)$$

Now, the continuity condition (3.4) ensures that $\hat{u}_n(X_j, t) = 0$ for $n > 0$, since $\hat{u}_0(X_j, t) = U_j(t) = u(X_j, t)$. Hence, we solve for d_j at $\xi = 0$ and c_j at $\xi = 1$, giving

$$\nu\hat{u}_1 = \sum_{j=1}^{N} \chi_j \left[\frac{H^2}{6}(\xi^3 + (1-\xi)^3\sigma^{-1} - \xi\Delta - \sigma^{-1})g_{1,j} \right.$$
$$\left. + \frac{\alpha H}{6}(\xi^3 + (1-\xi)^3\sigma^{-1} - \xi\Delta - \sigma^{-1})U_j.\Delta U_j \right]. \quad (4.9)$$

The value for $g_{1,j}$ can likewise be found from the smoothness condition (3.5), namely

$$\nu[\hat{u}_1']_j = -H\left(1 + \frac{1}{6}\delta^2\right)g_{1,j} - \alpha\left(1 + \frac{1}{6}\delta^2\right)U_j.\Delta U_j = -\frac{\nu\gamma}{H}\delta^2 U_j, \quad (4.10)$$

giving

$$g_{1,j} = \frac{\nu\gamma}{H^2}S\delta^2 U_j - \frac{\alpha}{H}U_j.\Delta U_j, \quad (4.11)$$

where $S^{-1} = 1 + \delta^2/6$.

such that

$$\frac{H^2}{6}\sigma(-\frac{3}{H}\sigma^{-1} - \frac{1}{H}(1-\sigma^{-1})g - \frac{H^2}{6}(\frac{3}{H} - \frac{1}{H}(1-\sigma^{-1}))g \qquad (4.12)$$

$$= \frac{H}{2}\sigma(-\sigma^{-1} - \frac{1}{3}(1-\sigma^{-1})g - \frac{H}{2}(1-\frac{1}{3}(1-\sigma^{-1}))g \qquad (4.13)$$

$$= \frac{H}{2}(-1 - \frac{1}{3}(\sigma-1)g - \frac{H}{2}(1-\frac{1}{3}(1-\sigma^{-1}))g \qquad (4.14)$$

$$= \frac{H}{2}(-2 + \frac{2}{3} - \frac{1}{3}\sigma - \frac{1}{3}\sigma^{-1})g \qquad (4.15)$$

$$= \frac{H}{2}(-2 - \frac{1}{3}\delta^2)g \qquad (4.16)$$

$$= -H(1 + \frac{1}{6}\delta^2)g \qquad (4.17)$$

5 Numerical stability

6 Conclusion

References

Fornberg, B. (1973), 'On the instability of the leap-frog and Crank–Nicolson approximations of a nonlinear partial differential equation', *Maths of Comput.* **27**, 45–57.

Roberts, A. J. (2001), 'Holistic discretisation ensures fidelity to Burgers' equation', *Applied Numerical Modelling* **37**, 371–396. doi:10.1016/S0168-9274(00)00053-2.
`http://arXiv.org/abs/chao-dyn/9901011`

Roberts, A. J. (2003), 'A holistic finite difference approach models linear dynamics consistently', *Mathematics of Computation* **72**, 247–262.
`http://www.ams.org/mcom/2003-72-241/S0025-5718-02-01448-5`

Roberts, A. J., MacKenzie, T. & Bunder, J. (2014), 'A dynamical systems approach to simulating macroscale spatial dynamics in multiple dimensions', *J. Engineering Mathematics* **86**(1), 175–207.
`http://arxiv.org/abs/1103.1187`